Photodynamic Properties of Dipeptide-Modified Hypocrellin B Derivatives: The Role of Tyrosine and Tryptophan Groups

Zhanghua Zeng,[†,‡] Rui Qiao,[†,‡] Jiahong Zhou,[†] Shengqin Xia,[†] Yan Zhang,[†] Yanyan Liu,[†,‡] Jinrong Chen,[†] Xuesong Wang,*[,†] and Baowen Zhang*[,†]

Laboratory of Organic Optoelectronic Functional Materials and Molecular Engineering, Technical Institute of Physics and Chemistry, Chinese Academy of Sciences, Beijing 100080, People's Republic of China, and Graduate School of Chinese Academy of Sciences, Beijing 100049, People's Republic of China

Received: September 26, 2006; In Final Form: December 25, 2006

Three long-wavelength absorbing dipeptide-modified hypocrellin B (HB) derivatives, Gly-HB, Tyr-HB, and Trp-HB, were prepared for application in photodynamic therapy (PDT). Their abilities to produce free radicals and singlet oxygen were compared in detail with EPR technique, and their binding interactions with calf thymus DNA (CT DNA) were studied by absorption spectra and DNA melting temperature measurements. Tyr-HB and Trp-HB distinguish themselves from Gly-HB and HB remarkably by their significantly improved efficiencies to generate semiquinone anion radicals, superoxide anion radicals, and hydroxyl radicals, as well as their affinity to CT DNA, as the result of the electron-donating properties and intercalating abilities of tyrosine and tryptophan groups. Tyr-HB and Trp-HB show remarkably enhanced photodamage capabilities on CT DNA than their parent HB in aerobic conditions. Moreover, they possess moderate photodamage abilities on CT DNA even in anaerobic conditions, indicating the role of Type I mechanism in their photodynamic behaviors.

1. Introduction

Photodynamic therapy (PDT) is a promising treatment modality for cancer and other nonmalignant conditions.[1−3] It involves the illumination of a photosensitizer with visible or near-infrared light, leading to the production of cytotoxic species. On the basis of the categories of the produced cytotoxic species, PDT can be classified into Type I and Type II in the photosensitization mechanism.[4] In the Type I mechanism, free radicals, generated through the electron and/or hydrogen (or proton) transfer between the excited photosensitizer and biomaterials, act as cytotoxic species, whereas in the Type II mechanism, the cytotoxic agent is singlet oxygen ($^1O_2$), which is produced by the energy transfer from the triplet excited state of photosensitizer to the ground state oxygen molecule.[5] In contrast to Type II, a highly oxygen-dependent process, Type I may still work at low O_2 concentration, and therefore may be a strategy to sustain photodynamic activity after the consumption of O_2 at the initial stage of PDT or to apply PDT in hypoxic conditions. For example, a porphyrin−fullerene dyad exhibited strong photodamage ability on the Hep-2 human-larynx-carcinoma cell line under argon, mainly due to the Type I mechanism as the result of efficient photoinduced intramolecular electron transfer in the dyad.[6]

Naturally occurring hypocrellins, including hypocrellin A (HA) and hypocrellin B (HB, Scheme 1), are well-known photodynamic sensitizers and their anticancer and antiviral activities have been scrutinized against a large variety of tumor cell lines and viruses.[7−10] Also, many novel hypocrellin derivatives were prepared to enhance the photodynamic activity by improving the absorptivity in the phototherapeutic window (600−900 nm),[11,12] tuning the hydrophilic−hydrophobic balance,[13,14] or increasing the affinity onto the biomolecules.[15,16] Recently, we synthesized a tyrosine-modified HB (TYHB, Scheme 1), and observed improved photodamage on calf thymus DNA (CT DNA) over its parent HB under both aerobic and anaerobic conditions.[17] The better photodynamic activity of TYHB may result from the intercalation ability of the tyrosine group, which increases the affinity of TYHB on CT DNA, and the electron-donating feature of the tyrosine group, which facilitates photoinduced intramolecular electron transfer and thus the Type I process. To understand further the role of the tyrosine group, we designed and synthesized three new dipeptide-modified HB derivatives (Scheme 1), with the dipeptide to be glycyl-glycin methyl ester (for Gly-HB), tyrosyl-glycin methyl ester (for Tyr-HB), or tryptophyl-glycin methyl ester (for Trp-HB), respectively. The dipeptides are linked, through 6-aminocaproic acid, to the HB skeleton both at C-2 by a C−N bond and at C-17 by a C═N bond. Such linking manners shift the absorption maxima of the resultant HB derivatives above 600 nm.[18] In contrast, the absorption maxima of HB and TYHB are 468 and 512 nm, respectively.[17] It was found that the presence of tyrosine or tryptophan renders Tyr-HB or Trp-HB higher generation abilities of semiquinone anion radicals, superoxide anion radicals ($O_2^{-\bullet}$), and hydroxyl radicals, and stronger photodamage on CT DNA. It is noteworthy that Tyr-HB and Trp-HB exhibit remarkable photodynamic activities under anaerobic conditions. We here report on the detailed comparison of the three dipeptide-modified HB derivatives in their generation efficiencies of free radicals and $^1O_2$, as well as their photodamage capabilities on CT DNA under both aerobic and anaerobic conditions, using HB or Cap-HB (aminocaproic acid-modified HB, the intermediate for preparation of the dipeptide-

* Address correspondence to this author. E-mail: g203@mail.ipc.ac.cn (B.Z.), xswang@mail.ipc.ac.cn X.W.). Phone: 86-01-82543592. Fax: 86-01-62554670.

† Technical Institute of Physics and Chemistry, Chinese Academy of Sciences.

‡ Graduate School of Chinese Academy of Sciences.

10.1021/jp066301y CCC: $37.00
Published on Web 03/22/2007

SCHEME 1: Chemical Structures of HA, HB, TYHB, Cap-HB, and Three Dipeptide-Modified HBs

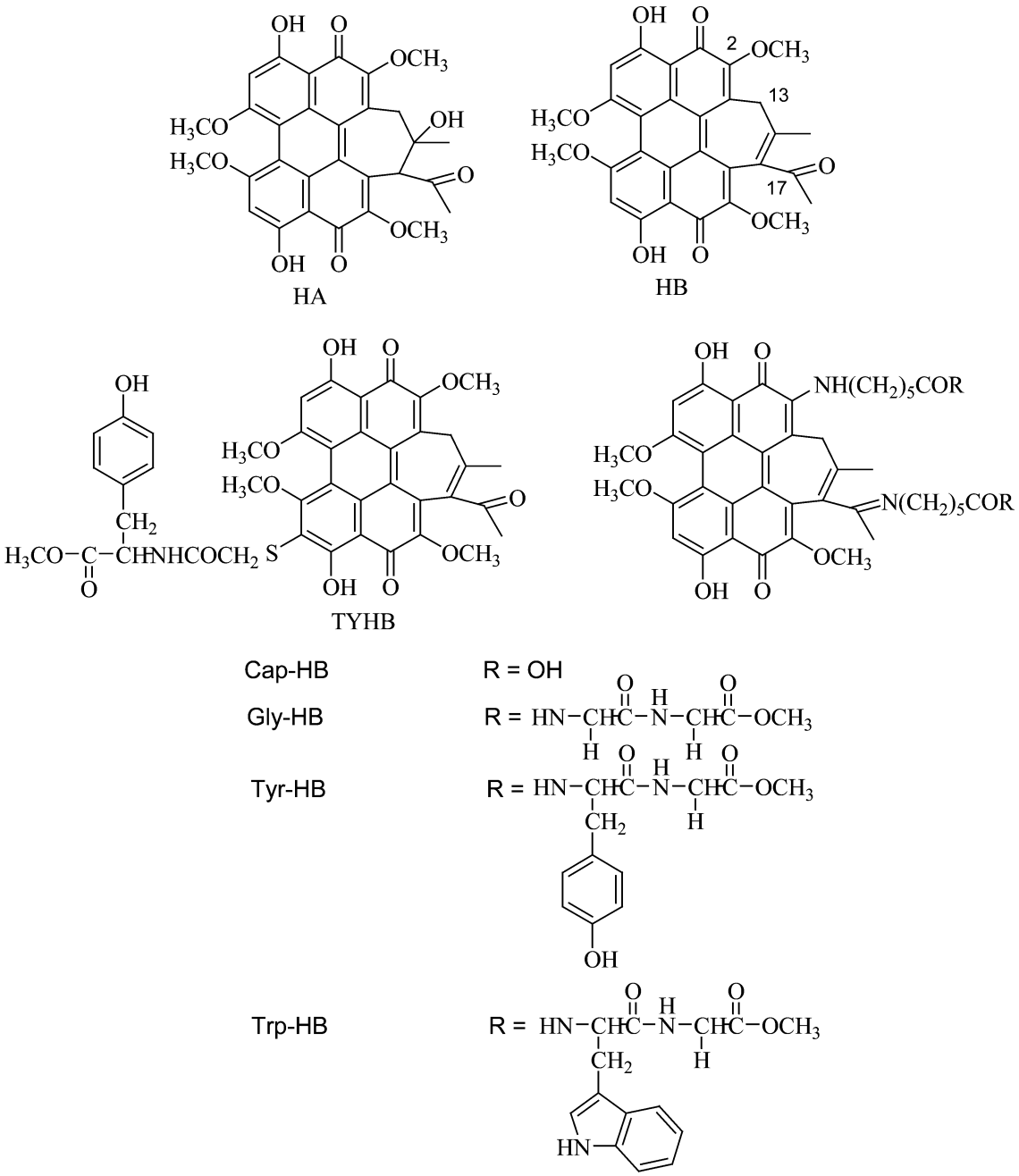

modified HBs, Scheme 1) as reference for elucidating the role of tyrosine or tryptophan groups.

2. Experimental Section

2.1. Chemicals. HA was isolated from fungus sacs of *hypocrella bambusae* and recrystallized three times from acetone before use. Ethidium bromide (EB), calf thymus DNA (DNA), and superoxide dismutase (SOD) were purchased from Sigma. 5,5-Dimethyl-1-pyrroline-*N*-oxide (DMPO), 2,2,6,6-tetramethyl-4-piperidone (TEMP), 9,10-diphenylanthracene (DPA), 1,4-diazabicyclo[2.2.2]octane (DABCO), and sodium azide (NaN_3) were purchased from Aldrich. Boc-L-tyrosine, Boc-L-tryptophan, and Boc-L-glycin were purchased from Fluka. *N*,*N*′-Dicyclohexylcarbodiimide (DCC) and *N*-hydroxybenzotriazole (HOBT) were purchased from Acros. *N*,*N*-Dimethylsulfoxide (DMSO) was dried over K_2CO_3 and distilled prior to use.

All experiments involving CT DNA were performed in PBS buffer solutions (pH 7.4) unless otherwise noted. CT DNA solutions were prepared by dispersing the desired amount of DNA in buffer solution with stirring overnight at temperatures below 4 °C. In the experiments where titration with DNA was required, the DNA solution was sonicated at 0 °C for 10 min, using a Brason probe ultrasonicator. This operation significantly reduced the viscosity of the DNA solutions and permitted more accurate and precise titration. The concentration of CT DNA was expressed as the concentration of nucleotide and was calculated by using an average molecular weight of 338 for a nucleotide and an extinction coefficient of 6600 $M^{-1}\cdot cm^{-1}$ at 260 nm.

2.2. Spectrum Measurements. UV−vis absorption spectra were recorded on a Shimadzu UV-1601 spectrophotometer. Fluorescence spectra were run on a Hitachi F-4500 fluorescence spectrophotometer. IR spectra were taken on a BIO-RAD FTS 165 grating spectrometer. ^1H NMR spectra were obtained on Varian GEMINI-300 and Bruker DMX-400 MHz spectrophotometers. Mass spectra were determined on a BIFLEXIII MALDI-TOF instrument.

2.3. Synthesis of the Dipeptide-Modified HBs. Caproic acid-modified HB (Cap-HB) and three dipeptide methyl esters were first prepared respectively following the reported method.[18] Then the condensation of Cap-HB (75 mg, 0.1 mmol) with corresponding dipeptide methyl ester (0.3 mmol) was carried out in CH_2Cl_2 in the presence of DCC (0.25 mmol) and HOBT (0.25 mmol) (in the dark, at room temperature, under N_2 atmosphere, for 24 h). After adding 0.5 mL of CH_3COOH to stop reaction and removal of the precipitate, the residue solution was subjected to column chromatography separation (1.5% KH_2PO_4 activated silica gel column with an eluent of chloroform/methanol in a volume ratio of 25:1) to obtain the aimed compounds.

Cap-HB: 20% yield with respect to HB. FT-IR (KBr, ν_{max}, cm^{-1}): 3410, 2990, 1733, 1612. ^1H NMR (300 MHz, d_6-DMSO, δ): 1.31 (m, 4H), 1.50−1.72 (m 11H), 2.20 (s, 3H), 2.30−2.43 (m, 4H), 2.60 (d, H-13a, J_{AB} = 11.2 Hz, 1H), 3.59 (d, H-13b, J_{AB} = 11.2 Hz, 1H), 3.88−3.97 (m, 4H), 4.03, (s, 3H), 4.09 (s, 3H), 4.14 (s, 3H), 6.33 (s, 1H), 6.79 (s, 1H), 12.77 (s, broad, 2H), 16.57 (s, 1H), 17.24 (s, 1H). MALDITOF−MS: 740.3 (M^+).

Gly-HB: 56% yield with respect to Cap-HB. FT-IR (KBr, ν_{max}, cm^{-1}): 3430, 3300, 1735, 1660, 1609. ^1H NMR (400 MHz, $CDCl_3$, δ): 1,26−1.42 (m, 4H), 1.73−1.78 (m, 11H), 2.16 (s, 3H), 2.22−2.34 (m, 4H), 2.61 (d, H-13a, J_{AB} = 13.5 Hz, 1H), 2.83 (s 4H), 3.51 (s, 4H), 3.59 (d, H-13b, J_{AB} = 13.5 Hz, 1H), 3.69 (s, 6H), 3.74−3.81 (m, 4H), 4.03 (s, 3H), 4.07 (s, 3H), 4.12 (s, 3H), 6.34 (s, 1H), 6.56 (s, 1H), 17.20 (s, 1H), 17.31 (s, 1H). MALDITOF−MS: 996.4 (M^+).

Tyr-HB: 47% yield with respect to Cap-HB. FT-IR (KBr, ν_{max}, cm^{-1}): 3470, 3280, 1730, 1670, 1610. ^1H NMR (400 MHz, $CDCl_3$, δ): 1.18−1.46 (m, 4H), 1.68−1.81 (m, 11H), 2.19 (s, 3H), 2.20−2.32 (m, 4H), 2.64 (d, H-13a, J_{AB} = 13.2 Hz, 1H), 2.93−3.05 (q, 4H), 3.55 (m, 4H), 3.61 (d, H-13b, J_{AB} = 13.2 Hz, 1H), 3.73 (s, 6H), 3.79−3.92 (m, 4H), 4.03 (s, 3H), 4.09 (s, 3H), 4.14 (s, 3H), 5.32 (q, 2H), 6.30 (s, 1H), 6.41(d, J_{AB} = 8.13 Hz, 4H), 6.49(d, J_{AB} = 8.13 Hz, 4H), 6.59 (s, 1H), 17.22 (s, 1H), 17.37 (s, 1H). MALDITOF−MS: 1208.5 (M^+).

Trp-HB: 41% yield with respect to Cap-HB. FT-IR (KBr, ν_{max}, cm^{-1}): 3410, 3280, 1745, 1665, 1612. ^1H NMR (400 MHz, $CDCl_3$, δ): 1.25−1.43 (m, 4H), 1.72−1.86 (m, 11H), 2.15 (s, 3H), 2.26−2.35 (m, 4H), 2.68 (d, H-13a, J_{AB} = 13.1 Hz, 1H), 3.37 (q, 2H), 3.52 (q, 2H), 3.59 (s, 4H), 3.68 (d, H-13b, J_{AB} = 13.1 Hz, 1H), 3.79 (s, 6H), 3.84−3.99 (m, 4H), 4.06 (s, 3H), 4.09 (s, 3H), 4.17 (s, 3H), 4.97 (q, 2H), 6.28 (s, 1H), 6.58 (s, 1H), 7.13−7.25 (m, 4H), 7.35 (s, 2H), 7.49 (d, J_{AB} = 8.9 Hz, 2H), 7.74 (d, J_{AB} = 8.6 Hz, 2H), 17.11 (s, 1H), 17.22 (s, 1H). MALDITOF−MS: 1254.5 (M^+).

2.4. $^1O_2$ Quantum Yield Measurements. The relative $^1O_2$ quantum yields were determined by the DPA bleaching method,[19] taking HB as reference. The photooxidation of DPA by photosensitizers was carried out on a "merry-go-round" apparatus, using a high-pressure mercury lamp (500 W) as the light source in combination with a 436 nm monochromatic filter. The optical densities at 436 nm of all samples were adjusted to the same. All samples were oxygen saturated and sealed prior to irradiation. The reactions were followed spectrophotometrically by observing the absorbance decrease of DPA at 374 nm (where the sensitizers used have the lowest absorption) as a function of irradiation time. The comparison of the absorbance decreasing rate during the initial period gave the relative quantum yields, assuming that of HB to be unity.

2.5. Free Radical Measurements by EPR. EPR spectra were obtained by using a Bruker ESP-300E spectrometer operating at room temperature, and the operating conditions were as follows: microwave bridge, X-band with 100 Hz field modulation; sweep width, 100 G; modulation amplitude, 1.0 G; modulation frequency, 100 kHz; receiver gain, 1×10^5; and microwave power, 5 mW. Samples were injected into the specially made quartz capillaries, and purged with argon, air, or oxygen for 30 min in the dark, respectively (the argon- and oxygen-saturated systems were sealed while the air-saturated systems were opened to the air), and illuminated directly in the cavity of the EPR spectrometer with a Nd:YAG laser (532 nm, 5−6 ns of pulse width, repetition frequency 10 Hz, 10 mJ/puse energy). The relative free radical quantum yields were estimated at normalized sample absorbance at 532 nm.

2.6. DNA Melting Temperature Measurements. The effects of the studied photosensitizers upon the melting temperature of CT DNA were measured by following the absorbance changes at 260 nm as a function of temperature. All the experiments were carried out by heating the CT DNA solutions from 25 to 90 °C at a rate of 1 deg/min in the absence or the presence of the concerned photosensitizer. The relative absorptions of A/A_0 (where A_0 and A are the absorbance at 260 nm at 25 °C and at a given temperature, respectively) were plotted against temperatures. The midpoints of the inflection region in the A/A_0 curves were taken as the corresponding melting temperature (T_m).[16]

2.7. Ethidium Bromide (EB) Assay for DNA Cleavage. A simple assay for DNA cleavage was applied based on ca. 20-fold enhancement of the fluorescence intensity exhibited by EB upon intercalation into DNA.[20,21] When the concentration of EB is two-fold higher than that of the DNA base pair, the fluorescence intensity of EB is linearly proportional to the concentration of the DNA base pair. Any process in which the potential EB binding site was destroyed results in a decrease in fluorescence intensity.

To a 10 mL EB/DNA buffer solution (80 μM EB, 40 μM CT DNA) was added the concerned photosensitizer to make the photosensitizer concentration 10 μM. Then the solution was divided into 5 aliquots and irradiated in a "merry-go-round" apparatus with a medium pressure sodium lamp ($h\nu$ > 470 nm). The aliquots were removed at various times and their fluorescence emissions in the range of 525−800 nm were measured by exciting at 510 nm.

The percentage of binding site remaining at a given time (t) was calculated from eq 1:

$$\%\ \text{binding site remaining} = 100 \times \left(1 - \frac{I_0 - I_t}{I_0 - I_{buffer}}\right) \quad (1)$$

where I_0, I_t, and I_{buff} denote the integrated fluorescence intensities before irradiation, after t min of irradiation, and of DNA-free buffer, respectively.

3. Results and Discussion

3.1. Photophysical Properties. Compared to HB, the absorption spectra of Cap-HB, Gly-HB, Try-HB, and Trp-HB show significant bathochromic shift (Figure 1 and Table 1).[22] The red shift is evidently the result of the substitution of the amino group for the methoxy group at C-2 of the parent HB and the formation of a Schiff base structure at C-17,[18] which increases greatly the absorbance of the resultant HB derivatives in the phototherapeutic window of 600−900 nm.

The absorption spectra of the three dipeptide-modified HBs overlap very well in the visible region with that of Cap-HB, suggesting a negligible interaction between HB moiety and dipeptide moiety in the ground state. However, the fluorescence

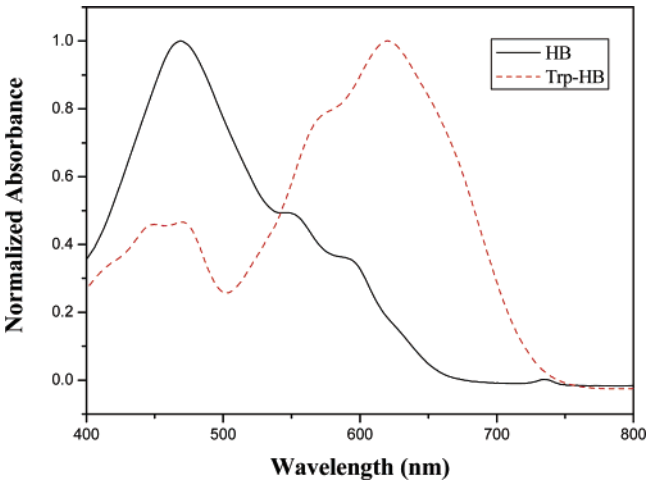

Figure 1. Normalized absorption spectra of HB and Trp-HB in CH_2Cl_2 solutions.

TABLE 1: Fluorescence Properties of HB, Cap-HB, and Three Dipeptide-Modified HBs in CH_2Cl_2

	λ^{ab}_{max} (nm)[a]	log ϵ (mol^{-1} cm^2)[b]	λ^{fl}_{max} (nm)[c]	Φ_f[d]
HB	465	4.11	604	0.22
Cap-HB	623	4.12	753	0.064
Gly-HB	622	4.08	752	0.051
Try-HB	620	4.06	752	0.019
Trp-HB	619	4.01	751	0.013

[a] Absorption maximum in CH_2Cl_2. [b] Extinction coefficient at absorption maximum. [c] Fluorescence maximum in CH_2Cl_2. [d] Fluorescence quantum yield in CH_2Cl_2 with HB as standard, whose fluorescence quantum yield in CH_3OH was measured to be 0.17.[22] The data are the average of three runs and the deviations are within ±10%.

emission intensity of Tyr-HB or Trp-HB is much lower than that of Cap-HB or Gly-HB (Table 1), indicating a strong quenching by the tyrosine or the tryptophan group. The quenching may mainly originate from the photoinduced intramolecular electron transfer (PET) from the tyrosine or the tryptophan group to the excited HB fraction. Taking the oxidation potentials (vs NHE) of 0.93 V for tyrosine and 0.80 V for tryptophan,[23,24] the reduction potential (vs NHE) of −0.64 V for Cap-HB (measured by cyclic voltammetry) and the 0−0 transition energy of 1.77 eV for Cap-HB, the free energy changes (ΔG) involved in PET are roughly estimated to be −0.2 eV in Tyr-HB and −0.33 eV in Trp-HB based on the Weller equation,[25] implying PET is thermodynamically permitted in both compounds. Thus, it is expected that Tyr-HB and Trp-HB should generate semiquinone anion radicals more efficiently upon excitation than Cap-HB and Gly-HB, which is really what we observed in EPR experiments (see below).

3.2. Generation of Semiquinone Anion Radical. HB is well-known for its ability to generate semiquinone anion radicals upon irradiation.[26] The semiquinone anion radicals are believed to result from the self-electron transfer, i.e., electron transfer between an excited HB (HB*) and a ground state HB (eq 2).[26]

$$HB^* + HB \rightarrow HB^{-\bullet} + HB^{+\bullet} \quad (2)$$

$$\text{Tyr (Trp)-HB}^* \rightarrow {}^{\bullet+}\text{Tyr } ({}^{\bullet+}\text{Trp})\text{-HB}^{-\bullet} \quad (3)$$

$$\text{Tyr (Trp)-HB}^* + \text{Tyr (Trp)-HB} \rightarrow \text{Tyr (Trp)-HB}^{-\bullet} + {}^{\bullet+}\text{Tyr } ({}^{\bullet+}\text{Trp})\text{-HB} \quad (4)$$

Irradiation of the argon-saturated DMSO solutions of Cap-HB and three dipeptide-modified HBs at 532 nm led to the

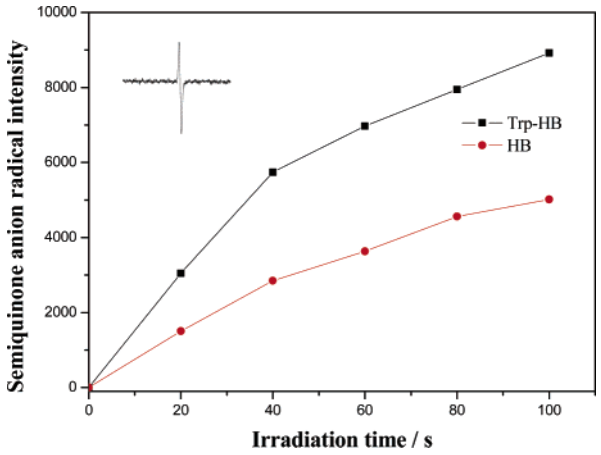

Figure 2. Dependence of the EPR signal intensity of semiquinone anion radical on irradiation time (irradiated at 532 nm) for argon-saturated DMSO solutions of HB (200 μM) and Trp-HB (200 μM). Inset: The EPR spectrum obtained for the irradiated solutions.

TABLE 2: Relative Quantum Yields of Semiquinone Anion Radical, $O_2^{-\bullet}$, and $^1O_2$ for HB, Cap-HB, and Three Dipeptide-Modified HBs

	$\Phi_{semiquinone}$[b]	$\Phi_{superoxide}$[c]	$\Phi_{singlet\ oxygen}$[d]
HB[a]	1.0	1.0	1.0
Cap-HB	0.9 ± 0.05	1.1 ± 0.1	0.3 ± 0.02
Gly-HB	0.9 ± 0.06	1.1 ± 0.1	0.3 ± 0.03
Tyr-HB	1.9 ± 0.1	2.2 ± 0.1	0.2 ± 0.02
Trp-HB	2.4 ± 0.1	2.9 ± 0.1	0.1 ± 0.01

[a] Assuming the corresponding quantum yield of HB to be unity. [b] In argon-saturated DMSO solutions. [c] In air-saturated DMSO solutions. [d] In oxygen-saturated DMSO solutions.

appearance of an EPR signal with the same position and line shape as that of the radical anion of HB (inset of Figure 2),[26] which indicates that these HB derivatives maintain the ability to generate semiquinone anion radicals as their parent HB. However, there are remarkable differences in the generation efficiencies. Figure 2 shows the relationships of the signal intensity of the semiquinone anion radicals with the irradiation time for HB and Trp-HB (the signal intensity changes vs irradiation time are very similar for other HB derivatives and therefore omitted in Figure 2 for clarity). During the initial period, the signal intensity increases linearly with irradiation time, and the slope represents the generation speed of semiquinone anion radical, from which the relative semiquinone quantum yields of the modified HBs with respect to HB (assuming its semiquinone quantum yield to be unity) can be estimated by correcting the absorption efficiency at 532 nm (Table 2). While the Cap-HB and Gly-HB generate semiquinone anion radicals with similar efficiency as HB, the relative semiquinone quantum yields of Tyr-HB and Trp-HB are ca. twice that of HB. For Tyr-HB and Trp-HB, the semiquinone anion radicals come not only from the self-electron transfer of the HB moiety (intermolecularly), but also from the electron transfer between the tyrosine or the tryptophan group and the HB moiety (inter- and intramolecularly, eqs 3 and 4). Due to the stronger electron-donating property of tryptophan over tyrosine, Trp-HB exhibits the highest efficiency to generate semiquinone anion radical among these HB derivatives. It will be shown below that the semiquinone anion radical generation efficiency controls the production of some reactive oxygen radicals such as superoxide and hydroxyl, and influences greatly the photodynamic activity in both aerobic and anaerobic conditions.

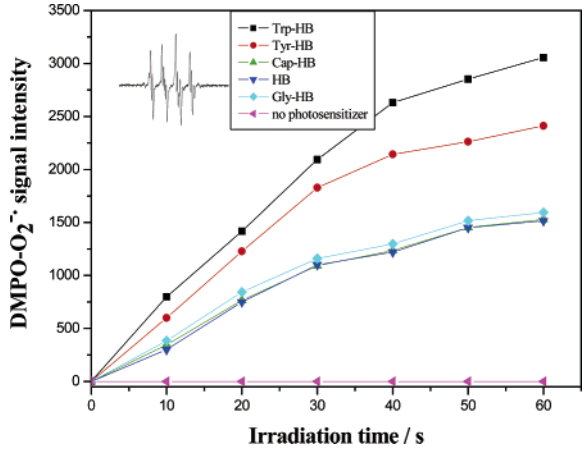

Figure 3. Dependence of the ESR signal intensity of DMPO−$O_2^{-\bullet}$ adduct on irradiation time (irradiated at 532 nm) for air-saturated DMSO solutions of HB, Cap-HB, and the three dipeptide-modified HBs (200 μM of photosensitizer) in the presence of 50 mM of DMPO. Inset: The ESR spectrum of DMPO−$O_2^{-\bullet}$ adduct obtained in the irradiated solutions.

In Figure 2, it is observed that the generation speed of the semiquinone anion radical declined to some extent after 40 s, which can be attributed to the increased disproportionation reaction of the netural semiquinone radical (i.e., the protonated semiquinone anion radical, with probably a trace amount of water as the proton source) at its higher concentration.[17,27,28]

3.3. Generation of Superoxide Anion Radical and Hydroxyl Radical. Upon introducing air or O_2 into the irradiated DMSO solutions of HB and its derivatives, the EPR signal intensity from semiquinone anion radicals was quenched significantly. With use of 5,5-dimethyl-1-pyrroline-*N*-oxide (DMPO) as the spin-trapping agent, a 12-line EPR spectrum with three hyperfine coupling constants of $\alpha^N = 13.0$ G, $\alpha_\beta^H = 10.1$ G, and $\alpha_\gamma^H = 1.5$ G and a *g* factor of 2.0056 was obtained (inset of Figure 3), which agrees well with the signal of the DMPO−$O_2^{-\bullet}$ adduct.[29] The presence of photosensitizer, oxygen, and light is essential for the generation of this EPR signal, and the addition of superoxide dismutase or *p*-benzoquinone, both the typical $O_2^{-\bullet}$ scavengers,[30] suppressed the signal intensity greatly. These control experiments confirm further the assignment of the signal to the DMPO−$O_2^{-\bullet}$ adduct. $O_2^{-\bullet}$ generated in these cases is believed to originate from the reduction of O_2 by the semiquinone anion radicals (eq 5, using HB as an example).[26]

$$HB^{-\bullet} + O_2 \rightarrow HB + O_2^{-\bullet} \quad (5)$$

Figure 3 gives the signal intensity of DMPO−$O_2^{-\bullet}$ adduct as the function of irradiation time. It is found again that the signal intensity increased at a lower rate after the initial irradiation period (ca. 30 s), which may be the result of the increased disproportionation reaction of the netural semiquinone radical as mentioned above and the consumption of O_2. Similar to the relative quantum yields for semiquinone anion radical, the relative quantum yields of $O_2^{-\bullet}$ are estimated as well based on the intensity increasing rates at the initial stages of the irradiation (Table 2). Evidently, there is a good correlation between the quantum yields of semiquinone anion radical and $O_2^{-\bullet}$, i.e., the higher efficiency to generate semiquinone anion radicals, the larger the relative quantum yield for $O_2^{-\bullet}$ production, suggesting again the origin of $O_2^{-\bullet}$ from semiquinone anion radicals.

When illumination with a 532 nm laser was carried out upon the air-saturated PBS buffer−DMSO (5:1 volume ratio) solutions of these HB derivatives in the presence of DMPO and a trace amount of Fe^{3+}, a new EPR spectrum was observed, which exhibit four lines with the intensity ratio of 1:2:2:1 that can be ascribed to twice splitting by the same hyperfine coupling constant of 14.9 G (Figure 4), suggesting the formation of a DMPO−hydroxyl adduct.[31] The observation of this signal needed the combination of photosensitizer, O_2, and light. Addition of sodium benzoate, a scavenger of hydroxyl,[32] quenched the signal noticeably. These findings further vindicate the assignment.

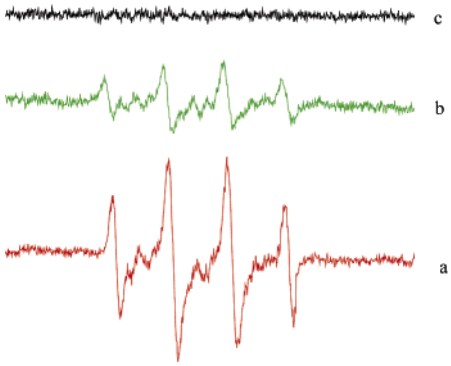

Figure 4. (a) EPR spectrum obtained upon irradiation (at 532 nm) of an air-saturated PBS buffer−DMSO (5:1) solution containing 20 mM of DMPO and 500 μM of Trp-HB. (b) Similar to part a, but in the presence of sodium benzoate (10 mM). (c) Similar to part a, but in the absence of Trp-HB, oxygen, DMPO, or light.

In aqueous solutions, $O_2^{-\bullet}$ from the reduction of O_2 by semiquinone anion radicals will transform into H_2O_2 easily by dispropotionation (eq 6) and/or further reduction by semiquinone anion radicals (eq 7). In the presence of redox active metals (e.g., Fe^{3+}), H_2O_2 will be further transformed into hydroxyl via the well-known Fenton reaction (eqs 8 and 9).[31] Also, the formation of hydroxyl can be realized by the reduction of H_2O_2 by semiquinone anion radicals (eq 10, taking HB as the example). These processes have been well accepted as the main pathways to generate hydroxyl for HA, HB, and their derivatives.[33] Both semiquinone anion radical and $O_2^{-\bullet}$ play key roles in these processes, and the formation of $O_2^{-\bullet}$ itself depends also on the semiquinone anion radical, therefore, it is not difficult to understand the stronger hydroxyl generation capabilities of Tyr-HB and Trp-HB than Gly-HB, Cap-HB, and HB.

$$O_2^{-\bullet} + O_2^{-\bullet} + 2H^+ \rightarrow H_2O_2 + O_2 \quad (6)$$

$$O_2^{-\bullet} + H^+ \rightarrow HO_2 + \text{semiquinone anion} + H^+ \rightarrow H_2O_2 \quad (7)$$

$$Fe^{3+} + O_2^{-\bullet} \rightarrow Fe^{2+} + O_2 \quad (8)$$

$$Fe^{2+} + H_2O_2 \rightarrow Fe^{3+} + OH^- + {}^\bullet OH \quad (9)$$

$$HB^{-\bullet} + H_2O_2 \rightarrow HB + OH^- + {}^\bullet OH \quad (10)$$

3.4. Generation of Singlet Oxygen. We used both spin-trapping and chemical-trapping techniques to compare the $^1O_2$ generation abilities of these HB derivatives. Figure 5a presents the EPR spectrum obtained upon irradiation of an oxygen-saturated DMSO solution of Trp-HB (200 μM) and TEMP (50 mM), in which TEMP acted as a spin-trapping agent for $^1O_2$.[34] The spectrum is composed of three equal-intensity lines with the hyperfine splitting constant of 16.0 G, identical with the typical EPR signal of TEMPO (adduct of TEMP with $^1O_2$).[33]

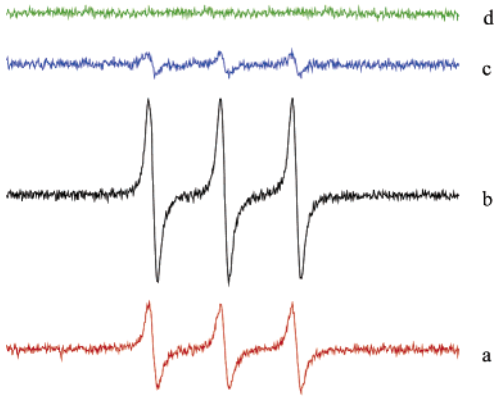

Figure 5. (a) EPR spectrum obtained upon irradiation (at 532 nm) of an O_2-saturated DMSO solution containing 50 mM TEMP and 200 μM Trp-HB. (b) Similar to part a, but in the d_6-DMSO solution. (c) Similar to part a, but in the presence of NaN_3 (10 mM). (d) Similar to part a, but in the absence of Trp-HB, oxygen, TEMP, or light.

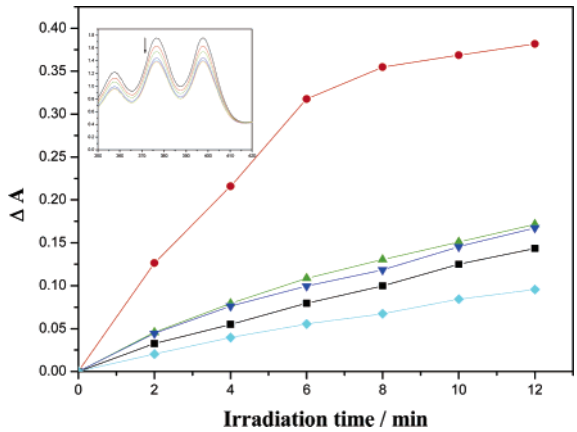

Figure 6. DPA bleaching at 374 nm as the function of irradiation time in oxygen-saturated DMSO solutions containing 30 μM photosensitizer and 100 μM DPA. The photosensitizers are respectively HB (●), Cap-HB (▲), Gly-HB (▼), Tyr-HB (■), and Trp-HB (◆). Inset: Absorption spectra of the DPA bleaching system at varied irradiation times. The arrow indicates the direction of changes.

This assignment is further supported by the fact that (1) any absence of Trp-HB, O_2, irradiation, and TEMP led to the disappearance of this signal (Figure 5d), (2) the presence of DABCO or NaN_3, both well-known scavengers for $^1O_2$, suppressed the signal markedly (Figure 5c), and (3) the signal intensity was about four times stronger in deuterated DMSO (Figure 5b). HB, Cap-HB, Gly-HB, and Tyr-HB exhibited similar behaviors when subjected to irradiation in the presence of TEMP and O_2.

The relative $^1O_2$ quantum yields of these HB derivatives were measured by using the 9,10-diphenylanthracene (DPA) bleaching method.[19] Figure 6 shows the absorbance changes at 374 nm as the function of irradiation time. The bleaching is due to the adduction of formed $^1O_2$ onto DPA, which is confirmed by the control experiments similar to those adopted in spin-trapping EPR experiments. In the case of HB, the bleaching rate began to decrease after ca. 6 min of irradiation. This phenomenon is in line with the higher $^1O_2$ generation efficiency of HB, which led to a more rapid consumption of O_2. In contrast, the $^1O_2$ quantum yields of Cap-HB, Gly-HB, Tyr-HB, and Trp-HB are much lower than that of HB (Table 2). Though the reason underlying the decreased $^1O_2$ generation efficiencies for Cap-HB and Gly-HB is not clear yet, the further decrease in $^1O_2$ quantum yields for Tyr-HB and Trp-HB may be attributed to the photoinduced intramolecular electron transfer, which quenches

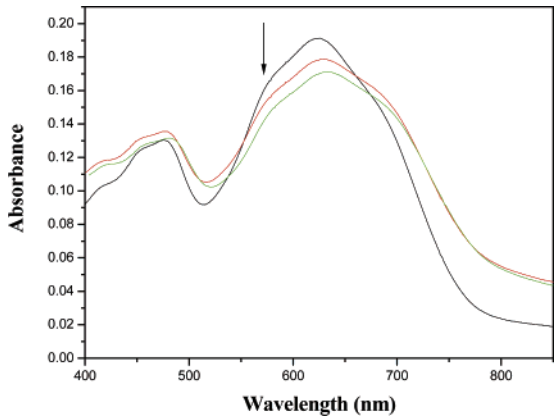

Figure 7. Absorption spectra of Trp-HB (10 μM) in phosphate buffer in the presence of increasing concentrations of CT DNA (0, 40, and 100 μM, respectively).

the triplet excited state and thus interferes with the triplet energy transfer to ground state O_2.

In summary, the photoinduced intramolecular electron transfer renders Tyr-HB and Trp-HB much higher efficiencies to generate semiquinone anion radicals, superoxide anion radicals, and hydroxyl radicals. The $^1O_2$ quantum yields of Tyr-HB and Trp-HB, however, are lower than that of HB. In our experimental conditions, we did not observe EPR signals coming from cation radicals such as $HB^{+\bullet}$, mainly due to their short lifetimes.[35]

3.5. Affinity to CT DNA. Tyrosine and tryptophan belong to amino acids bearing aromatic residues. This kind of amino acid possesses a special ability to intercalate partially into the double helix DNA.[36] Our previous work showed that a tyrosine-modified HB (TYHB, Scheme 1) exhibited binding interactions with CT DNA in the ground state.[17] Therefore, the UV−visible absorption spectrum and DNA melting temperature measurement were applied to investigate the mutual interactions between CT DNA and these new HB derivatives.

Figure 7 shows the absorption spectrum changes of Trp-HB solution in phosphate buffer upon titration of CD DNA. The addition of 100 μM of CT DNA led to a red shift of the absorption maximum by 3.5 nm and an absorbance decrease at the absorption maximum (hypochromism) by 12%. Tyr-HB underwent absorption changes to a similar extent, i.e., bathochromic shift by 3.0 nm and hypochromism by 10% in the presence of 100 μM CT DNA. The binding constants were measured to be 3.63×10^3 and 5.88×10^3 M^{-1} respectively for Tyr-HB and Trp-HB.[37] In contrast, the changes are negligible in the cases of HB, Cap-HB, and Gly-HB. Obviously, the presence of the tyrosine or the tryptophan group enhances the interactions of the HB moiety with CT DNA, very likely due to the intercalating capability by which the photosensitizer is tethered to the double helix.

It is expected that the interactions between photosensitzer and CT DNA should also influence the properties of DNA itself to some extent. This is supported by DNA melting temperature measurements. The melting temperature of CT DNA in phosphate (1 mM) buffer (pH 7.0) in the presence of 10 mM NaCl was measured at 61 °C. The presence of Tyr-HB or Trp-HB (20 μM) gave rise to a decrease of 3−4(±0.5) °C in the melting temperature of CT DNA, while no observable melting temperature changes were found in the cases of HB, Cap-HB, and Gly-HB, indicating further the role of tyrosine and tryptophan groups in improving the affinity of the corresponding HB derivatives to CT DNA.

TABLE 3: Photocleavage of CT DNA by HB, Cap-HB, and Three Dipeptide-Modified HBs Detected by the Remaining Binding Site (BSR%) of Ethidium Bromide to the Damaged CT DNA under Different Conditions ([CT DNA] = 40 μM, [EB] = 80 μM, [photosensitizer] = 10 μM)

	BSR% at varied irradiation				
samples	10 min	20 min	30 min	40 min	50 min
control experiment[a]	99.0	98.1	96.7	96.1	95.3
HB + O_2[b]	81.8	73.4	66.5	61.3	58.4
Cap-HB + O_2[b]	80.3	70.1	63.7	58.9	55.7
Gly-HB + O_2[b]	80.2	70.5	63.6	57.9	51.4
Tyr-HB + O_2[b]	70.5	61.3	48.8	34.6	29.7
Trp-HB + O_2[b]	61.7	47.8	33.1	20.8	15.2
HB + argon[c]	96.8	93.5	91.3	89.4	87.3
Cap-HB + argon[c]	96.9	93.1	89.0	86.5	84.1
Gly-HB + argon[c]	94.3	89.7	86.2	83.8	81.5
Tyr-HB + argon[c]	90.8	85.4	80.7	74.9	72.6
Trp-HB + argon[c]	88.0	80.4	77.6	73.1	69.2

[a] Without photosensitizer and in air-saturated buffer. [b] In air-saturated buffer. [c] In argon-saturated buffer.

3.6. Photodamage on CT DNA. The photodynamic activities of these HB derivatives were compared by using CT DNA as the target. Table 3 lists the results of EB assay under both aerobic and anaerobic conditions. After 50 min of irradiation in aerobic conditions, the binding sites (for EB intercalation on CT DNA) remained 58.4% for HB, 55.7% for Cap-HB, and 51.4% for Gly-HB, in great contrast to 29.7% for Tyr-HB and 15.2% for Trp-HB. We also compared the photodamage abilities of Trp-HB and HB toward supercoiled pBR322 plasmid DNA. The higher photocleavage activity of Trp-HB was observed, evidenced by electrophoresis analyses (see the Supporting Information). It has been shown that Cap-HB and Gly-HB have similar abilities to generate semiquinone anion radial, superoxide anion radical, and hydroxyl radical, but decreased singlet oxygen quantum yields with respect to HB (Table 2). Thus, the slightly increased photodamage abilities (on CT DNA) of Cap-HB and Gly-HB may be the result of their red-shifted absorption spectra from HB (Table 1), since irradiations were performed with a continuum light above 470 nm (from a medium pressure sodium lamp). But we cannot exclude the possibility that Cap-HB and Gly-HB bind somewhat more tightly to CT DNA than the parent HB, though the binding, if any, should be very weak for all of them as aforementioned. The further significant improvements of the photodamage abilities of Tyr-HB and Trp-HB are evidently due to the presence of tyrosine and tryptophan groups. The modification of HB by tyrosine or tryptophan, on one hand, leads to increased production of free radical species such as semiquinone anion radicals, superoxide anion radicals, and hydroxyl radicals, and thus more contributions to photodamage from the Type I mechanism. On the other hand, the presence of the tyrosine or the tryptophan group renders the corresponding HB derivative better affinity to CT DNA, thus favoring the reactive species to attack the target (the short lifetimes of the reactive species necessitate their proximity to the target biomolecules). The combination of the two factors may account for the much improved photodynamic activities of Tyr-HB and Trp-HB in aerobic conditions.

The role of the Type I mechanism in the photodynamic behaviors of Tyr-HB and Trp-HB can be reflected more clearly in anaerobic conditions. If a photosensitizer can generate only singlet oxygen via the Type II mechanism, its photodynamic activity should be diminished in an oxygen-deficient environment. In the cases of HB and its derivatives studied here, photodamage of CT DNA was still found in anaerobic conditions, though the damage extents were decreased more than in aerobic conditions. The decreased photodamage extents in argon-saturated solutions may be ascribed to the lacking of the Type II mechanism and/or the lacking of O_2 in free radicals propagation (through superoxide, peroxide, or hydroxyl). It is worth noting that Tyr-HB and Trp-HB, particularly the later, exhibited moderate photodamage abilities in this case, implying the importance of the Type I mechanism. Besides the semiquinone anion raidicals, the tyrosine or tryptophan derived primary cation radicals (obtained upon donating an electron to the excited HB moiety) and their secondary radical species may also damage the DNA structures,[38] considering both tyrosine and tryptophan groups can intercalate into the base pairs of the double helix.

4. Conclusions

Three long-wavelength-absorbing dipeptide-modified HB derivatives, Gly-HB, Tyr-HB, and Trp-HB, were compared thoroughly with HB and Cap-HB, a 6-aminocaproic acid-substituted HB, in terms of absorption, fluorescence, and generation abilities of semiquinone anion radicals and other reactive oxygen species, as well as the photodamage on CT DNA. The electron-donating properties of tyrosine and tryptophan groups make Tyr-HB and Trp-HB more efficient to generate semiquinone anion radicals and other oxygen-based radicals (superoxide anion radicals and hydroxyl radicals). Meanwhile, the intercalating abilities of tyrosine and tryptophan groups render Tyr-HB and Trp-HB affinities to CT DNA. Thus, Tyr-HB and Trp-HB exhibited much stronger damage to CT DNA than HB, Cap-HB, and Gly-HB in both aerobic and anaerobic conditions. The moderate photodynamic activities of Tyr-HB and Trp-HB in argon-saturated systems suggest that it is of importance to develop novel photosensitizers, that can work under the Type I mechanism, for PDT applications in hypoxic conditions.

Acknowledgment. This work was supported by the Chinese Academy of Sciences (project no. KJCX2.YW.H08).

Supporting Information Available: Electrophoreses gel pattern of supercoiled pBR322 DNA upon irradiation in the presence of HB or Trp-HB. This material is available free of charge via the Internet at http://pubs.acs.org.

References and Notes

(1) Dougherty, T. J. *Photochem. Photobiol.* **1993**, *58*, 895.
(2) Detty, M. R.; Gibson, S. L.; Wagner, S. J. *J. Med. Chem.* **2004**, *47*, 3897.
(3) MD, M. A. A. *Clin. Dermatol.* **2006**, *24*, 16.
(4) Oschsner, M. J. *Photochem. Photobiol.* **1997**, *39*, 1.
(5) Foote, C. S. *Photochem. Photobiol.* **1991**, *54*, 145.
(6) Milanesio, M. E.; Alvarez, M. G.; Rivarola, V.; Silber, J. J.; Durantini, E. N. *Photochem. Photobiol.* **2005**, *81*, 891.
(7) Duran, N.; Song, P. S. *Photochem. Photobiol.* **1986**, *61*, 677.
(8) Diwu, Z. J. *Photochem. Photobiol.* **1995**, *61*, 529.
(9) Kraus, G. A.; Zhang, W.; Fehr, M. J.; Petrick, J. W.; Wannemuehler, Y.; Carpenter, S. *Chem. Rev.* **1996**, *96*, 523.
(10) Hudson, J. B.; Imperial, U.; Hauglan, R. P.; Diwu, Z. J. *Photochem. Photobiol.* **1997**, *65*, 352.
(11) Wu, T.; Xu, S. J.; Shen, J. Q.; Song, A. M.; Chen, S.; Zhang, M. H. *Anticancer Drug Des.* **2000**, *15*, 287.
(12) Xu, S. J.; Chen, S.; Zhang, M. H.; Tao, S. *Biochim. Biophys. Acta* **2000**, *6*, 1523.
(13) Zhao, Y. W.; Xie, J.; Ma, J. S.; Zhao, J. Q. *New J. Chem.* **2004**, *28*, 484.
(14) Ou, Z. Z.; Chen, J. R.; Wang, X. S.; Zhang, B. W.; Cao, Y. *New J. Chem.* **2001**, *25*, 847.
(15) Zhou, J. H.; Xia, S. Q.; Chen, J. R.; Wang, X. S.; Zhang, B. W. *Chem. Commun.* **2003**, 1372.
(16) Zhou, J. H.; Liu, J. H.; Xia, S. Q.; Chen, J. R.; Wang, X. S.; Zhang, B. W. *J. Phys. Chem. B* **2005**, *109*, 19529.

(17) Xia, S. Q.; Zhou, J. H.; Chen, J. R.; Wang, X. S.; Zhang, B. *Chem. Commun.* **2003**, 2931.
(18) Lee, H. Y.; Chen, S.; Zhang, M. H.; Shen, T. *J. Photochem. Photobiol., B* **2003**, *71*, 43.
(19) Diwu, Z. J.; Lown, J. W. *J. Photochem. Photobiol., A* **1992**, *64*, 273.
(20) Pruetz, W. A. *Radiat. Environ. Biophys.* **1984**, *23*, 1.
(21) LePecq, J. B.; Paoletti, C. *J. Mol. Biol.* **1967**, *27*, 87.
(22) Liu, J. Y.; Zhang, M. H.; An, J. Y. *Photogr. Sci. Photochem.* **1986**, *1*, 36.
(23) Slobodan, V. J.; Anthony, H.; Michael, G. S. *J. Phys. Chem.* **1986**, *90*, 1935.
(24) Weng, M.; Zhang, M. H.; Shen, T. *J. Chem. Soc., Perkin Trans.* **1997**, *2*, 2393.
(25) Kavarnos, G. J.; Turro, N. J. *Chem. Rev.* **1986**, *86*, 401.
(26) Hu, Y. Z.; An, J. Y.; Jiang, L. J.; Chen, D. W. *J. Photochem. Photobiol., A* **1995**, *89*, 45.
(27) Pal, H.; Palit, D. K.; Mukherjee, T.; Mittal, J. P. *Radiat. Phys. Chem.* **1991**, *37*, 227.
(28) Mukherjee, T.; Land, E. J.; Swallow, A. J.; et al. *J. Chem. Soc., Faraday Trans.* **1988**, *84*, 2855.
(29) Harbour, J. R.; Hair, M. L. *J. Phys. Chem.* **1978**, *82*, 1397.
(30) (a) McCord, J. M.; Fridovich, I. *J. Biol. Chem.* **1969**, *244*, 6049. (b) Manring, L. E.; Kramer, M. K.; Foote, C. S. *Tetrahedron Lett.* **1984**, *25*, 2523.
(31) Lang, K.; Wagnerova, M.; Stopka, P.; Dameran, W. *J. Photochem. Photobiol., A* **1992**, *67*, 187.
(32) Gomes, A.; Fernandes, E.; Lima, J. L. F. C. *J. Biochem. Biophys. Methods* **2005**, *65*, 45.
(33) Hu, Y. Z.; Jiang, L. J. *J. Photochem. Photobiol., B* **1996**, *33*, 51.
(34) Lion, Y.; Delmelle, M.; Vorst, A. V. *Nature* **1976**, *263*, 442.
(35) Mayer, J.; Krasluklanis, R. *J. Chem. Soc., Faraday Trans.* **1991**, *87*, 2943.
(36) Gabbay, E. J.; Sanford, K.; Baxter, C. S.; Kapicak, L. *Biochemistry* **1973**, *21*, 1240.
(37) (a) Kumar, C. V.; Asuncion, E. H. *J. Am. Chem. Soc.* **1993**, *115*, 8547. (b) Modukuru, N. K.; Snow, K. J.; Perrin, B. S., Jr.; Thota, J.; Kumar, C. V. *J. Phys. Chem. B* **2005**, *109*, 11810.
(38) Hawkins, C. L; Davies, M. J. *Biochim. Biophys. Acta* **2001**, *1504*, 196.